

AUTHOR QUERY FORM

 ELSEVIER	Journal: JBMT Article Number: 13429	Please e-mail or fax your responses and any corrections to: E-mail: corrections.esco@elsevier.tnq.co.in Fax: +31 2048 52789
--	--	---

Dear Author,

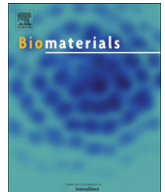
Please check your proof carefully and mark all corrections at the appropriate place in the proof (e.g., by using on-screen annotation in the PDF file) or compile them in a separate list. To ensure fast publication of your paper please return your corrections within 48 hours.

For correction or revision of any artwork, please consult <http://www.elsevier.com/artworkinstructions>.

Any queries or remarks that have arisen during the processing of your manuscript are listed below and highlighted by flags in the proof.

Location in article	Query / Remark: Click on the Q link to find the query's location in text Please insert your reply or correction at the corresponding line in the proof
Q1	Please note that there is a discrepancy in the authors names in the list and citaion [28].
Q2	Please confirm that given names and surnames have been identified correctly.

Thank you for your assistance.



Repairing critical-sized calvarial defects with BMSCs modified by a constitutively active form of hypoxia-inducible factor-1 α and a phosphate cement scaffold

Q2 Duohong Zou^{a,b,c,1}, Zhiyuan Zhang^{b,1}, Jiakai He^{c,1}, Siheng Zhu^c, Shaoyi Wang^b, Wenjie Zhang^b, Jian Zhou^c, Yuanjin Xu^b, Yan Huang^d, Yuanyin Wang^c, Wei Han^e, Yong Zhou^b, Shuhong Wang^a, Sulan You^f, Xinquan Jiang^{b,**}, Yuanliang Huang^{f,*}

^aSchool of Stomatology, Tongji University, Shanghai 200011, China

^bOral Bioengineering Lab/Regenerative Medicine Lab, Department of Prosthodontics, Shanghai Research Institute of Stomatology, Ninth People's Hospital Affiliated with Shanghai Jiao Tong University, School of Medicine, Shanghai Key Laboratory of Stomatology, Shanghai 200011, China

^cDepartment of Oral and Maxillofacial Surgery, School of Stomatology, Stomatological Hospital, Anhui Medical University, Hefei 230032, China

^dDepartment of orthodontics, the Affiliated Hospital of Medical College Qingdao University, China

^eDepartment of Oral and Maxillofacial Surgery, Nanjing Stomatological Hospital, Nanjing 210008, China

^fDepartment of Stomatology, Shanghai East Hospital Affiliated with Tongji University, 150 Jimo Road, Shanghai 200011, China

ARTICLE INFO

Article history:

Received 20 August 2011

Accepted 1 September 2011

Available online xxx

Keywords:

HIF-1 α

BMSCs

Calcium–magnesium phosphate cement

Osteogenesis

ABSTRACT

Tissue engineering combined with gene therapy represents a promising approach for bone regeneration. The Hypoxia-inducible factor-1 α (HIF-1 α) gene is a pivotal regulator of vascular reactivity and angiogenesis. Our recent study has showed that HIF-1 α could promote osteogenesis of bone mesenchymal stem cells (BMSCs) using a gene point mutant technique. To optimize the function of HIF-1 α on inducing stem cells, another constitutively active form of HIF-1 α (CA5) was constructed with truncation mutant method and its therapeutic potential on critical-sized bone defects was evaluated with calcium-magnesium phosphate cement (CMPC) scaffold in a rat model. BMSCs were treated with Lenti (lentivirus)–CA5, Lenti-WT (wild-type HIF-1 α), and Lenti-LacZ. These genetically modified BMSCs were then combined with CMPC scaffolds to repair critical-sized calvarial defects in rats. The results showed that the overexpression of HIF-1 α obviously enhanced the mRNA and protein expression of osteogenic markers *in vitro* and robust new bone formation with the higher local bone mineral density (BMD) was found *in vivo* in the CA5 and WT groups. Furthermore, CA5 showed significantly greater stability and osteogenic activity in BMSCs compared with WT. These data suggest that BMSCs transduced with truncation mutant HIF-1 α gene can promote the overexpression of osteogenic markers. CMPC could serve as a potential substrate for HIF-1 α gene modified tissue engineered bone to repair critical sized bony defects.

© 2011 Published by Elsevier Ltd.

1. Introduction

Due to inflammatory disease, trauma, and anatomical or congenital conditions, bone defects are quite common and pose a substantial clinical and biomedical burden. Researches in tissue engineering have shown that tissue engineering combined with gene therapy represents a promising approach for bone regeneration [1]. The previous experiments demonstrate that many factors, such as bone morphogenic protein (BMP), vascular endothelial

growth factor (VEGF), and fibroblast growth factor (bFGF), can stimulate osteogenesis and angiogenesis in bone defects using local gene therapy method [2,3].

Some studies have reported that hypoxia-inducible factor-1 α (HIF-1 α) could promote the expression of angiogenic genes. HIF-1 α has widely been regarded as a critical regulator during angiogenic–osteogenic coupling [4]. Hypoxia-inducible factor (HIF)-1 is a transcription factor that mediates the adaptation of many multicellular organisms to molecular oxygen [5]. It includes two subunits: O₂-regulated α and constitutively-expressed β . HIF-1 α is the specific subunit of HIF-1 that determines its biological activity [6]. Several hundreds of genes have been determined to be regulated directly by HIF-1, including VEGF and stromal-derived factor 1 (SDF-1) [7]. Hydroxylation of proline residues 402 and 564 and asparagine residue 803 in HIF-1 α regulates protein stability and

* Corresponding author. Tel.: +86 21 38804518; fax: +86 21 58765119.

** Corresponding author. Tel.: +86 21 23271132.

E-mail addresses: xinquan@yahoo.cn (X. Jiang), Yuanlianghuangyx@126.com (Y. Huang).

¹ These authors contributed equally to this work.

transactivation function in an O₂-dependent manner [5,8–11]. Based on these data, Lenti-CA5, a lentivirus encoding a mutant form of HIF-1 α , was constructed in this study. Truncation mutant was made by a deletion (amino acids 392–520) and two substitutions (Pro567Thr and Pro658Gln). Lenti-CA5 is resistant to O₂-dependent degradation and maintains constitutive activity under non-hypoxic conditions [12]. As multipotent stem cells, bone marrow-derived mesenchymal stem cells (BMSCs) are ideal seed cells for Tissue engineering [11]. In many previous reports, many factors can enhance mesenchymal stem cells (MSCs) osteogenesis and angiogenesis, such as BMP, runt-related transcription factor 2 (Runx2), and VEGF [13–15]. HIF-1 α , as an upstream gene that regulates their transcription, has many advantages including vascular remodeling and bone repair compared with the above genes. Our previous study has indicated that point mutant HIF-1 α (proline 564 to alanine, proline 402 to alanine and aminosuccinic acid 803 to alanine) could increase BMSC expression levels of osteogenic genes *in vitro* in the normoxic condition [16]. To optimize the function of HIF-1 α on inducing stem cells, CA5 (a constitutively active form of HIF-1 α) was constructed with truncation mutant method to verify whether the CA5 modified BMSCs could achieve an enhanced activity of osteogenesis in tissue engineering in this study?

As a key factor for bone tissue engineering, scaffold should provide sufficient mechanical support and a three-dimensional space for cell proliferation, osteogenic differentiation, and consequent bone formation *in vivo* [17,18]. Comparing to organic scaffold material, such as a collagen and gelatin scaffold, nonorganic scaffold material including CPC, β -TCP, usually possesses sufficient mechanical strength and stiffness to enable stress transfer and load bearing [19]. Among those nonorganic scaffolds, calcium phosphate biomaterials have been widely used in clinical applications because of their excellent biocompatibility and osteoconductivity [20,21]. Comparing to calcium phosphate cement (CPC, low biodegradation rate [22,23]), calcium–magnesium phosphate cement (CMPC) was fabricated by incorporating magnesium oxide into CPC to improve both mechanical and degradation properties [24,25]. Besides, magnesium added in CPC may enhance osteoblast adhesion, and thus directly stimulate osteoblast proliferation, and indirectly influence new bone formation [26]. CMPC exhibits good biocompatibility, biodegradability and osteoconductivity [27].

Based on the above knowledge, applying a combination of CMPC scaffolds and BMSCs modified by Lenti-CA5 treatment appears to be

a promising approach to repair bone defect. In this paper, we tested the hypothesis that CA5 gene therapy could be used to promote the repair of critical-sized defect (CSD) in a rat skull model using CMPC scaffold.

2. Materials and methods

2.1. Isolation and culture of rat BMSCs

Animal use was compliant with official Chinese guidelines and was assessed by the local Internal Evaluation Committee for Animal Welfare and Rights. Total BMSCs were isolated from a 6-week-old male Fisher 344 rats with a weight of 50 g \pm 5 g according to the protocol reported by Xinquan Jiang et al. [28]. Briefly, primary cells were cultured in Dulbecco's modified Eagle's medium (DMEM) (Gibco BRL, Grand Island, NY, USA) containing 10% FBS and 100 units/mL penicillin for 5 days. The medium was then changed and was renewed three times a week. When 90% confluence was reached, BMSCs were released from the culture substratum using trypsin/EDTA (0.25% w/v trypsin, 0.02% EDTA) and moved to dishes (10 cm in diameter) at 1.0×10^5 cells/mL in 10 mL at 37 °C in an atmosphere of 5% CO₂. Flow cytometry was used to characterize BMSCs with CD90, CD105, CD31, and CD34 staining (Invitrogen, Carlsbad, California, USA).

2.2. Lenti-CA5 construction and BMSCs gene transduction

Lenti-WT is a replication-defective lentivirus that encodes enhanced green fluorescent protein (EGFP) and HIF-1 α . The HIF-1 α in Lenti-CA5 is constitutively active as a result of a deletion (amino acids 392–520) and two substitutions (Pro567Thr and Pro658Gln), as previously described [7]. Large-scale lentiviral production was performed in the Shanghai R&S Biotechnology Co., Ltd. BMSCs were exposed to 15 MOI of Lenti-WT, Lenti-CA5, or EGFP-encoding lentiviral vector (Lenti-LacZ) for 24 h in the presence of polybrene (8 μ g/mL). Transduction efficiency, which was assessed by counting the number of EGFP-positive cells after 4 days of culture.

2.3. Real-time quantitative RT-PCR analysis

Total cellular RNA extraction of BMSCs was performed on days 0, 1, 4, 7, 14, and 21 after gene transduction with an RNeasy Mini kit (Qiagen, Germany). The quality and quantity of the RNA obtained were checked by spectrophotometric analysis using the biophotometer (Eppendorf biophotometer plus). According to the manufacturer's recommendations, reverse transcription was finished with 1 μ g of total RNA in a final volume of 20 μ L, using a PrimeScript RT reagent kit (Takara Bio, Shiga, Japan). The relative expression of each target mRNA was calculated using the comparative ΔC_t method with 18S rRNA as the reference [29]. The gene-specific primers were synthesized commercially (Shengong Co., Ltd., Shanghai, China), and the genes, accession numbers, primer sequences, and amplicon sizes are listed in Table 1. All values were normalized to GAPDH. All experiments were performed in triplicate; results are reported as the average \pm SD.

2.4. Western blotting analyses

Cells (1.0×10^5 /well) were seeded onto 6-well plates 1 day before transduction. Total protein was harvested from cultured cells on days 0, 1, 4, 7, 14, and 21 after gene

Table 1
Nucleotide sequences for real-time RT-PCR primers.

Genes	Primer sequence (5'-3') (Forward/reverse)	Product size (bp)	Annealing temperature (°C)	Accession number
Osteonectin	CCCTACTATGTCGCTTCTTGG GTTTCGTGCTTGTATGGG	199	60	NM_001530.3
Glut1	GCTTCTGCTCATCAATCGTAAC TCATCTGCCGACCCCTCTCT	168	60	NM_138827.1
COL1	TCCTGCCGATGTCGCTATC CAAGTTCGGGTGACTCCGTG	234	58	XM_213440
OCN	CAGTAAGGTGGTGAATAGACTCCG GGTGCCATAGATGCGCTTG	172	60	NM_013414.1
BMP-2	GCGTGCTTCTAGACGGACTG CGTCAGAGGGCTGGGATG	158	60	NM_017178.1
BSP	TGGATGAACCAAGCGTGGA TCGCCTGACTGTCGATAGCA	162	60	NM_012881.2
ALP	GTCCACAAGAGCCACAAT CAACGGCAGAGCCAGGAAT	172	60	NM_013059.1
Cbfa1	TCTTCCAAAGCCAGAGCG TGCCATTTCGAGGTGGTCCG	154	60	NM_053470.1
OPN	TGGATGAACCAAGCGTGGA TCGCCTGACTGTCGATAGCA	168	60	NM_012881.2
GAPDH	GGCAAGTTCAACGGCACAGT GCCAGTAGACTCCACGACAT	76	60	NM_017008.3

transduction. The procedure was performed according to standard protocols. Briefly, after cells lysed, protein concentrations were measured using the DC protein assay kit (Invitrogen, Carlsbad, California, USA). Equal amounts of cell lysates were separated on duplicate 8–10% SDS-PAGE gels and transferred to a polyvinylidene difluoride (PVDF) membrane (0.45 μm , Millipore, Bedford, MA). The membranes were incubated with specific primary antibodies (HIF-1 α , Abcam, Inc., Cambridge, UK) overnight at 4 °C at a 1:600 dilution. The membranes were then washed three times with TBS containing 0.1% tween-20 detergent and incubated for 2 h with HRP-conjugated secondary antibodies. Protein bands were visualized using the Enhanced Chemiluminescence system (Amersham Pharmacia Biotech Inc., USA) and Kodak X-OMAT film (Rochester, New York, USA). The same procedure was used for antibodies against other proteins, including BMP-2, osteocalcin (OCN), osteopontin (OPN), and sialoprotein (BSP) (Abcam, Inc., Cambridge, UK). Relative protein levels were normalized against β -actin. All experiments were performed in triplicate. Results are reported as the mean \pm SD.

2.5. Alkaline phosphatase activity and alizarin red-S staining

BMSCs/Lenti-WT, BMSCs/Lenti-CA5, or BMSCs/Lenti-LacZ were plated on 6-well plates at a density of 1.0×10^5 cells/well and were cultured in DMEM until they were confluent. Next, they were evaluated for alkaline phosphatase (ALP) activity and Alizarin Red-S Staining (ARS) on days 14 and 21 after transduction. The semi-quantitative analyses of ALP and ARS were performed following an established protocol [30]. Briefly, after cells lysed, the total protein content of these samples was determined using the BCA method with a protein assay kit (Rockford, Ill). ALP activity was determined at 405 nm using p-nitrophenyl phosphate (pNPP) (Sigma–Aldrich, St. Louis, Mo. USA) as the substrate. For ARS measurements, after cells were washed and fixed, the samples were then stained with ARS (40 mM) for 20 min at room temperature. The stain was desorbed with 10% cetylpyridinium chloride (Sigma–Aldrich, St. Louis, Mo. USA) for 1 h. The solution was collected and distributed at 100 μL /well on a 96-well plate, and absorbance readings were taken at 590 nm using a spectrophotometer (Thermo Spectronic, California, USA). Finally, ALP and ARS levels were normalized to the total protein content. All experiments were conducted in triplicate.

2.6. Preparation of BMSCs/CMPC constructs

CMPC scaffolds (East China University of Science and Technology, Shanghai, China) were molded into cylinders (Φ 5 mm \times 2 mm³) and sterilized by ⁶⁰Co irradiation before use. The scaffolds had an average pore size of 400 μm \pm 50 μm and 75% porosity. For cell seeding, BMSCs were detached from culture dishes, centrifuged to remove supernatant, and then resuspended in the serum-free DMEM at a density of 2.0×10^5 cells/mL. Cells in suspension were slowly added to the CMPC cylinder till final saturation. After incubation for an additional 4 h to allow for cell attachment, the scaffolds were used as described in next section.

In a parallel experiment, 3 mm \times 3 mm \times 3 mm cuboids were prepared and seeded with BMSCs at an identical cell density. At the 4 h and 24 h time points, the constructs were fixed in 2% glutaric dialdehyde for 2 h, cut into two halves, and then characterized by scanning electron microscopy (Philips SEM XL-30, Amsterdam, Netherlands).

2.7. Animal experiments

All procedures were approved by the Ninth People's Hospital Affiliated with Shanghai Jiao Tong University Committee on the Use and Care of Animals. Surgical procedures were performed on a 12-week-old male Fisher 344 rats, as described previously [31]. Briefly, the animals were anaesthetized by intraperitoneal injection of pentobarbital (Nembutal 3.5 mg/100 g). A 1.0- to 1.5-cm sagittal incision was made on the scalp, and the calvarium was exposed by blunt dissection. Two critical-sized defects were created by means of a 5-mm diameter trephine bur (Fine Science Tools, Foster City, CA, USA). Twenty-four rats with two critical-sized calvarial defects were generated and randomly allocated into the following graft study groups: (1) CMPC ($n = 6$); (2) CMPC with BMSCs/Lenti-LacZ ($n = 6$); (3) CMPC with BMSCs/Lenti-WT ($n = 6$); and (4) CMPC with BMSCs/Lenti-CA5 ($n = 6$). The incision was closed in layers using 4–0 resorbable sutures. The rats were able to function normally after this procedure.

2.8. Sequential fluorescent labeling

The polychrome sequential labeling of mineralizing tissues was performed according to a previous report [32]. At 1, 4, and 7 weeks after the operation, the animals were subjected to intraperitoneal injection of fluorochromes under ether anesthesia as follows: tetracycline hydrochloride (1 mg/kg body weight, TE, Sigma–Aldrich, St. Louis, Mo. USA), calcein (1% in 2% NaHCO₃ solution, 5 mL/kg body weight, CA, Sigma–Aldrich, St. Louis, Mo. USA), Alizarin Red-S (3% in 2% NaHCO₃ solution, 0.8 mL/kg body weight, AL, Sigma–Aldrich, St. Louis, Mo. USA).

2.9. Radiography and micro-CT measurement

At 8 weeks post-operation, all the rats were sacrificed by an intraperitoneal overdose injection of pentobarbital. The skulls were then explanted and fixed in 4%

phosphate-buffered formalin solution. X-ray images of skulls were made with a Kodak In-Vivo Imaging System FX Pro. Calvarial samples were placed near the center of the FOV of the phosphor screen. X-ray images were acquired using radiographic screens.

The morphology of the reconstructed skulls was assessed using an animal micro-CT scanner (eXplore Locus, GE Healthcare Biosciences, London, UK). As previously reported [33], briefly, the specimens were scanned with some parameters, including an X-ray tube potential of 80 kV, a tube current of 0.45 mA, and 15- μm voxel resolution. After micro-CT scan, the visualization of bone was made with software of three-dimensional isosurface renderings. Micro-CT measurements included bone mineral densities (BMDs) and the trabecular thickness (Tb.Th) in the bone defect.

2.10. Histological and histomorphometric observation

The samples were fixed in a 5% neutral buffered formalin solution. The undecalcified specimens of 12 rats (half of the specimens for each group, $n = 6$) were dehydrated in ascending concentrations of alcohols from 75% to 100% and finally embedded in polymethylmetacrylate (PMMA). The orientation of the sections was selected on the sagittal surface in each animal. Three sections, representing the central area of each defect, were used for the histometric analysis. The specimens were cut in 150 mm thick sections using a microtome (Leica, Hamburg, Germany) and were subsequently polished to a final thickness of about 40 μm [34]. Sections were observed for fluorescent labeling using a confocal laser scanning microscope (CLSM) (Leica TCS Sp2 AOBs, Heidelberg, Germany). The excitation/emission wavelengths of the chelating fluorochromes used were 405/560–590 nm (tetracycline, yellow), 488/500–550 nm (calcein, green), 543/580–670 nm (Alizarin Red-S, red) respectively [35]. Then the sections were stained with Van Gieson's picro fuchsin for histological observation. To analyze mineralization in the skull, the fluorochrome staining of the new bone was quantified using the methodology of Wang et al. [36]. The microscope images were stored digitally and then evaluated histomorphometrically using a picture-analysis system (Image-Pro Plus™, Media Cybernetic, Silver Springs, MD, USA). Using this system, the number of pixels labeled with each fluorochrome in each image was determined as a percentage of the mineralization area. This analysis was performed separately for yellow (tetracycline, TE), green (calcein, CA), and red (Alizarin Red-S, AL). The data on tetracycline, calcein and Alizarin Red-S staining represent the bone regeneration and mineralization 1, 4, and 7 weeks post-operation.

The measurements on areas of newly formed bone and remnant scaffold were quantified using a personal computer-based image analysis system (Image Pro 5.0, Media Cybernetic, Silver Springs, MD, USA) and reported as a percentage of the whole bone defect area.

2.11. Immunohistochemistry

The samples of another half of each group ($n = 6$) were decalcified in 10% EDTA for 2 weeks. Samples were embedded in paraffin, and serial coronal cross sections were made. Immunohistochemistry was performed as previously described [28]. Briefly, the tissue slides were dewaxed and rehydrated, after which endogenous peroxidase activity was blocked using 3% (w/v) hydrogen peroxide (H₂O₂) in methanol for 30 min, and slides were blocked using the avidin/biotin blocking kit (Vector Laboratories, Inc., Peterborough, UK) and incubation in Tris Buffered Saline (TBS), supplemented with 5% BSA and 20% normal serum (NS). Primary antibodies against GFP and HIF- α (1:100 dilution) (Abcam, Inc., Cambridge, UK) were diluted in 5% BSA/TBS and applied to the sections at 4°C overnight. The biotinylated secondary antibody (Boster Co. Ltd., Shanghai, China) was applied to the slides for 30 min at room temperature. Then, streptavidin biotin complex (Boster Co. Ltd., Shanghai, China) was incubated for 20 min. Staining was performed by DAB substrate (DAKO, Cambridge, UK), and the slides were counterstained with hematoxylin and mounted.

2.12. Statistical analysis

All data are presented as the mean \pm SD. Using the software SPSS 10.0 (SPSS Science), statistical significance was assessed by a Tukey's *post-hoc* test of ANOVA. A P -value < 0.05 was considered statistically significant (* $P < 0.05$ and ** $P < 0.01$, target gene (WT or CA5) groups compared with the control group; # $P < 0.05$ and ## $P < 0.01$, the CA5 group compared with the WT group).

3. Results

3.1. Cell culture and characterization of BMSCs

After rat bone marrow was extracted, it was cultured in uncoated dishes in DMEM with 10% FBS to isolate BMSCs. By passages 3–5, BMSCs were detached, and then the flow cytometry was analyzed. As previously described for MSCs [37], BMSCs showed high expression of CD90 and CD105, whereas myeloid

endothelial cell marker CD31 and hematopoietic marker CD34 were rarely detected (Supporting Information, Fig. S1).

3.2. Gene transduction and HIF-1 α expression

After CA5 mutation (Supporting Information, Fig. S2), Lenti-WT and Lenti-CA5 were produced. For optimal multiplicity of infection (MOI), a set of preliminary experiments was performed using various doses of lentivirus. Finally, we found that a MOI of 15 resulted in optimal transduction efficiency without excessive cell death *in vitro*. Four days after transduction, approximately 90% of BMSCs were observed to be green using inverted fluorescence microscopy (Supporting Information, Fig. S3). Overexpression of HIF-1 α was detected in the Lenti-WT and Lenti-CA5 groups by RT-PCR and western blotting (Fig. 1).

3.3. RT-qPCR and western blot analysis of osteogenic markers

To detect expression of osteogenic genes in BMSCs, RT-qPCR was carried out on days 0, 1, 4, 7, 14, and 21. Levels of pivotal osteogenic factors were obviously different among the various groups. In target gene-transduced BMSCs, the expression of BMP-2 and Cbfa1, which are regarded as important factors in regulating bone formation, was increased markedly on day 4 and improved continuously from day 7 to day 21 (Fig. 2A and B). BMP-2 displayed remarkably increase in the HIF-1 α -transduced groups. Other pivotal osteogenic genes such as ALP, OCN, OPN, and Glut1 showed the same tendency as BMP-2 and Cbfa1

(Fig. 2C–E and H). However, BSP and type I collagen (COL1) demonstrated notable upregulation from day 7 (Fig. 2F and G). Furthermore, osteonectin was not upregulated until later, on day 14 (Fig. 2I). In comparison, the transcripts of osteogenic markers in the LacZ group remained at a low level after 21 days. Taken together, these data support the presence of an osteoinductive effect induced by CA5.

To detect protein expression of osteogenic factors in the gene-modified BMSCs, we chose four pivotal factors. The results of analyzing various protein levels were in accordance with the qPCR data (Fig. 3A). After gene transduction, BMP-2 was detected on days 0, 1, 4, 7, 14, and 21 in the Lenti-WT-, Lenti-CA5-, and LacZ-transduced groups. Quantitative analysis revealed an 8- to 10-fold increase in the Lenti-WT- and Lenti-CA5-transduced groups (Fig. 3B-a). In addition, we investigated whether OCN, OPN, and BSP were also upregulated *via* the HIF-1 pathway. The results showed that the expression of OCN was increased 3- to 4-fold in the target gene-transduced group compared to the LacZ group (Fig. 3B-b). Similar results were observed for OPN and BSP (Fig. 3B-c and d). These data indicated that CA5 could enhance the expression of osteogenic proteins in BMSCs *in vitro*.

3.4. ALP and ARS

Lenti-WT-, Lenti-CA5-, and LacZ-transduced BMSCs were plated on 6-well plates (10^5 cells/well). On days 14 and 21 after gene transduction, ALP staining was obviously enhanced in target gene-transduced groups (Fig. 4A). Furthermore, ARS staining on

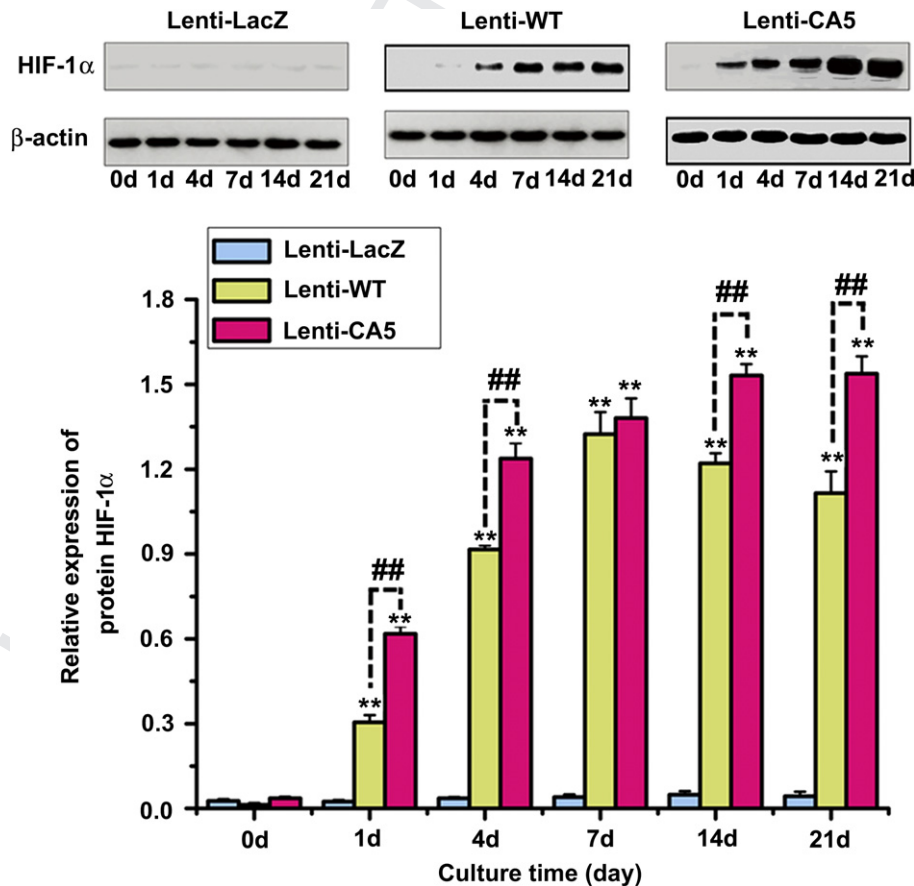


Fig. 1. The protein expression of HIF-1 α was determined using western blot. BMSCs transduced with Lenti-WT and Lenti-CA5 produced a higher level of HIF-1 α compared with Lenti-LacZ-transduced BMSCs (** $P < 0.01$, target gene groups compared with the control group; ## $P < 0.01$, the CA5 group compared with the WT group).

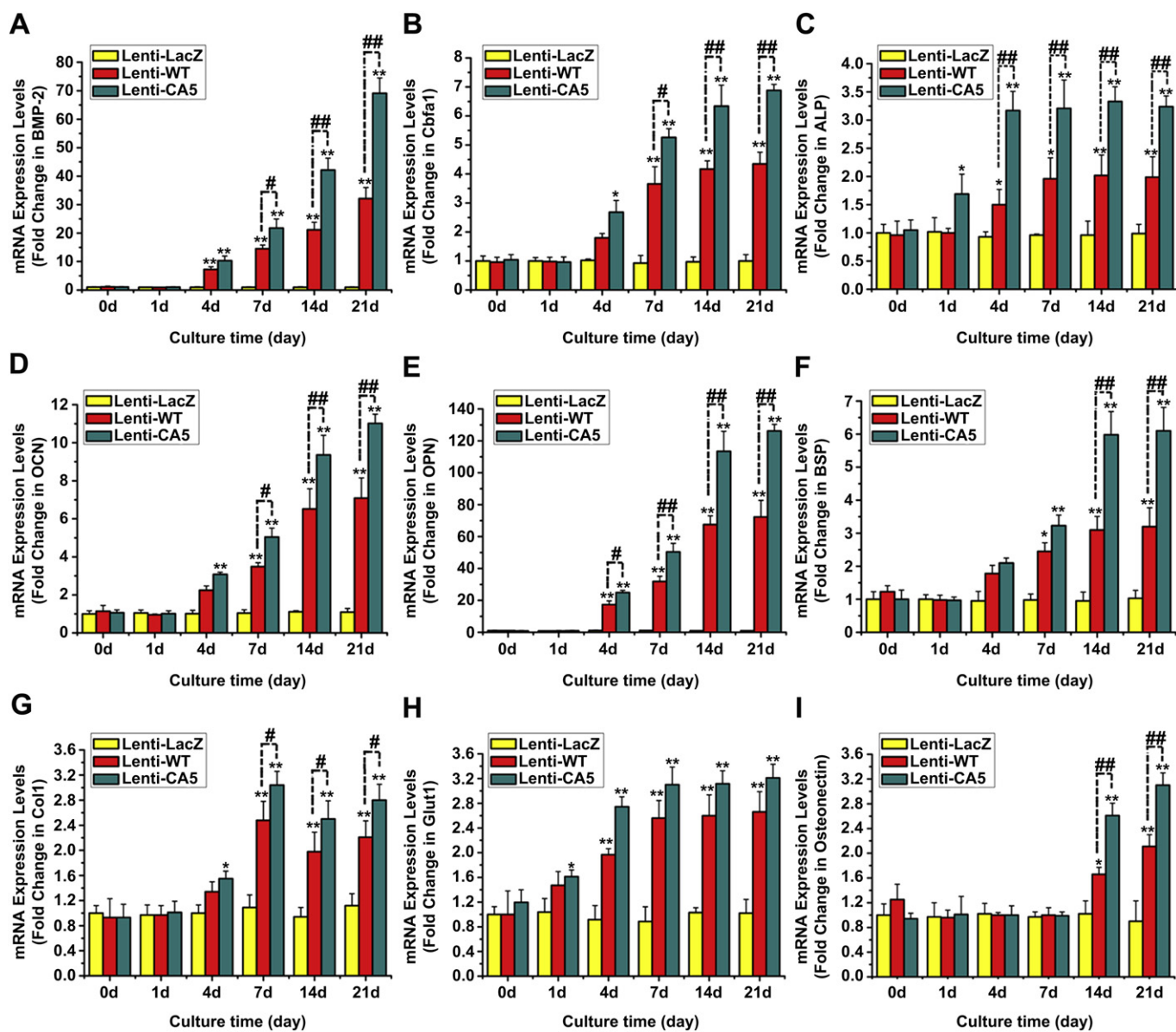


Fig. 2. Detection of mRNA expression of osteogenic markers in rat BMSCs. mRNA expression of BMP-2 (A) Cbfa1 (B) ALP (C) OCN (D) OPN (E) BSP (F) COL1 (G) Glut1 (H) and osteonectin (I) (* $P < 0.05$ and ** $P < 0.01$, target gene groups compared with the LacZ group; # $P < 0.05$ and ## $P < 0.01$, the CA5 group compared with the WT group).

day 21 revealed a significant increase in calcium deposition (Fig. 4C). The semi-quantitative analysis showed that ALP activity in Lenti-WT or Lenti-CA5 groups was 3.2-fold greater than the control group on day 21. There was also a statistical difference between the Lenti-WT and Lenti-CA5 groups (Fig. 4B). In addition, the semi-quantitative analysis of ARS agreed with the result for ALP (Fig. 4D). However, there was no statistical difference between the Lenti-WT and Lenti-CA5 groups until day 21. All these results proved that HIF-1 α could promote the differentiation of BMSCs into osteoblastic cells.

3.5. Adhesion of BMSCs on scaffold and the implant procedure

The CMPC scaffold was evaluated by scanning electron microscope (Supporting Information, Fig. S4A). 24 h after the BMSCs were combined with the material, cells attached to the surface of the scaffold *in vitro* (Supporting Information, Fig. S4B). Nominal differences in cellular adhesion and proliferation were observed

between BMSCs transduced with LacZ, WT, CA5, and untransduced BMSCs. After 4 h the scaffolds combined with BMSCs, the compounds (CMPC; CMPC with BMSCs/Lenti-LacZ; CMPC with BMSCs/Lenti-WT; and CMPC with BMSCs/Lenti-CA5) were placed into the critical-sized calvarial defects (Supporting Information, Fig. S4C and D).

3.6. Radiographic analysis and micro-CT measurement

To observe new bone formation within the defects, X-ray images were taken at 8 weeks after explantation of the skull. Representative photographs of each group are shown in Fig. 5A. Radiographic evidence of new bone formation was highly variable among the four groups. In the Lenti-WT and Lenti-CA5 groups, new bone formation was seen, and the appearance of the implant became smoother and more radiopaque. However, there were more radiopaque areas in the CMPC and Lenti-LacZ groups, especially the CMPC group.

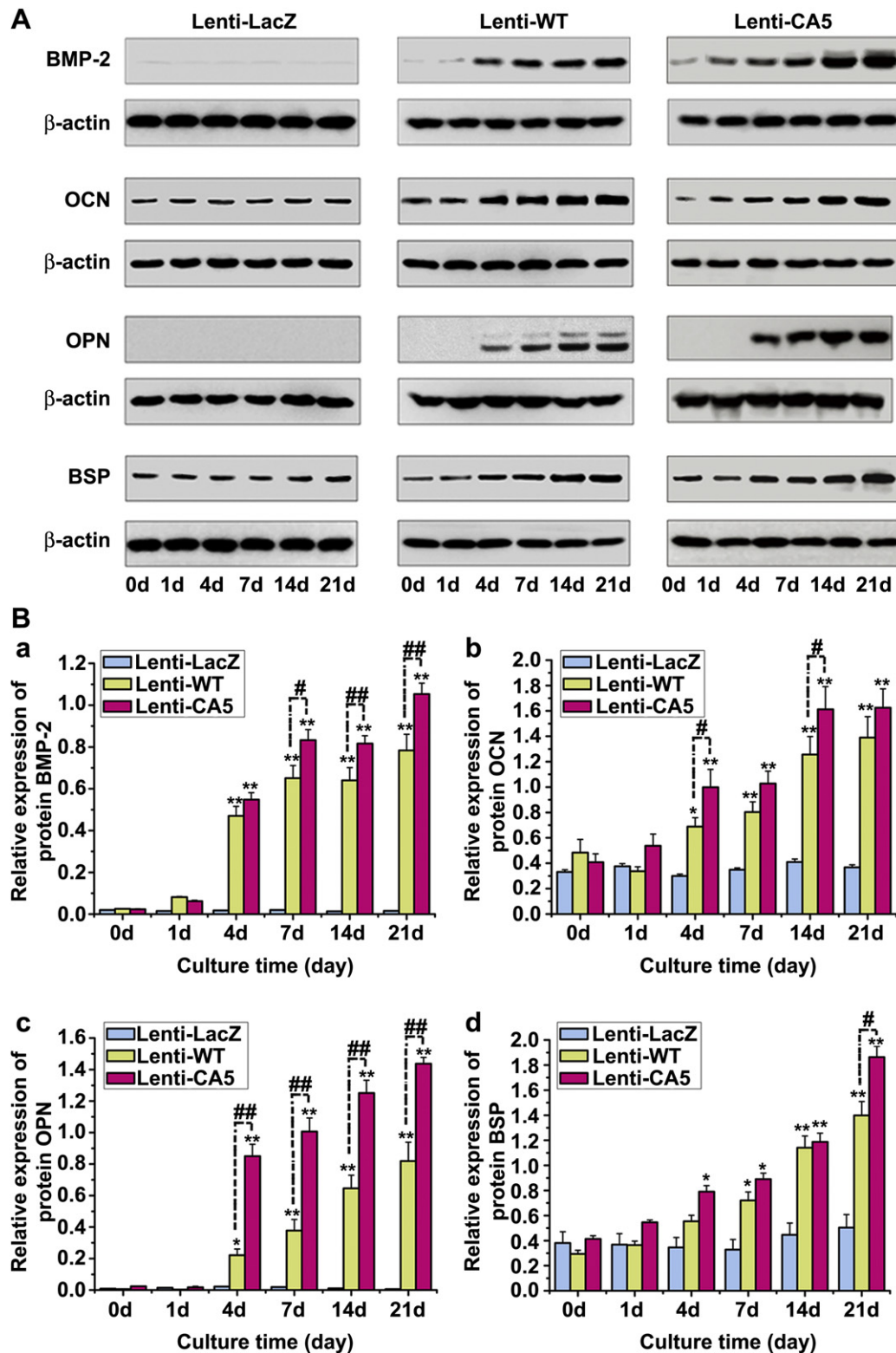


Fig. 3. Expression of osteogenic markers was detected by western blot. (A) Grayscale scan showed that after gene transduction, BMP-2, OCN, OPN, and BSP proteins were expressed in BMSCs on days 0, 1, 4, 7, 14, and 21. (B) Scan Image software detected gray values of the BMP-2, OCN, OPN, and BSP proteins band at different time points. All values were normalized to β -actin ($^*P < 0.05$ and $^{**}P < 0.01$, target gene groups compared with the LacZ group or CMPC group; $^{\#}P < 0.05$ and $^{\#\#}P < 0.01$, the CA5 group compared with the WT group).

The morphology of the newly formed bone was reconstructed using micro-CT. The results were nearly in conformity with the X-ray images. From coronal to sagittal, micro-CT showed that the new bone formation in the target gene groups was greater than that in

the LacZ or CMPC groups at 8 weeks post-operation (Fig. 5B). The quantity of the newly formed bone in the defect sites was calculated by morphometrical analysis. Significantly greater BMD was observed in the Lenti-WT- and Lenti-CA5-transduced BMSCs

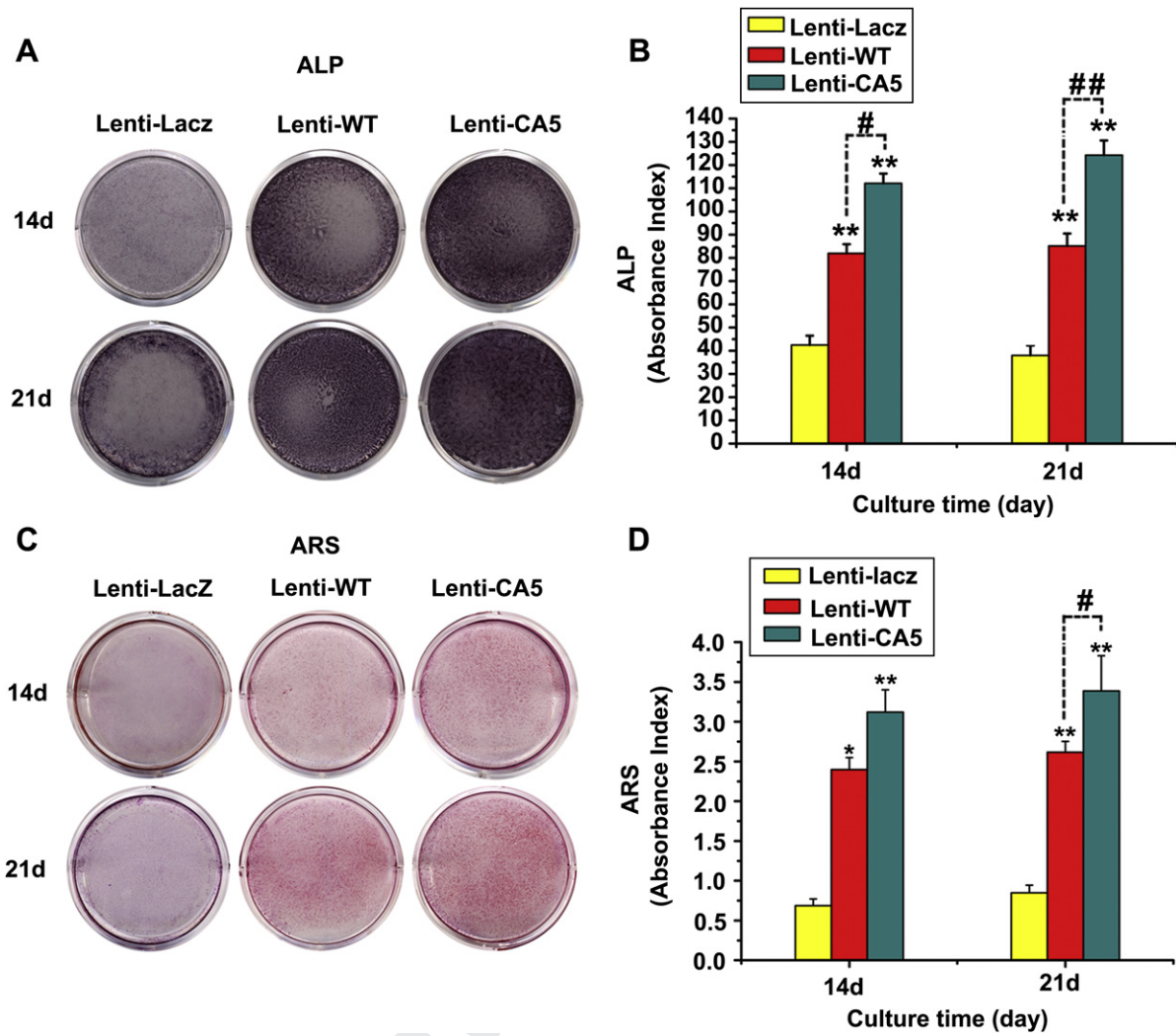


Fig. 4. Analysis of ALP and ARS staining. ALP expression on days 14 and 21 (A) Semi-quantitative analysis of ALP activity (B) The results of ARS staining (C) Semi-quantitative analysis of ARS (D) (* $P < 0.05$ and ** $P < 0.01$, target gene groups compared with the LacZ group or CMPC group; # $P < 0.05$ and ## $P < 0.01$, the CA5 group compared with the WT group).

groups (Fig. 5C). Tb.Th of the Lenti-WT- and Lenti-CA5-transduced BMSCs groups were also higher than in the other two groups (Fig. 5D).

3.7. Fluorochrome labeling histomorphometrical analysis

New bone formation and mineralization were determined histomorphometrically by TE, CA, and AL fluorescent quantification, which represented the mineralization level at different time periods. At 1 week, the percentage of TE labeling (yellow) in the Lenti-WT group was $3.18 \pm 0.43\%$, which was greater than the percentage in the CMPC group of $1.69 \pm 0.51\%$ or the LacZ group of $1.82 \pm 0.54\%$, but less than the percentage in the Lenti-CA5 group of $4.57 \pm 0.87\%$ ($P < 0.01$; Fig. 6A-a1, b1, c1, d1, and B). At 4 weeks, the percentage of CA labeling (green) was $1.62 \pm 0.38\%$, $2.0 \pm 0.49\%$, $9.24 \pm 1.24\%$, and $10.67 \pm 1.54\%$, for Groups CMPC, LacZ, WT, and CA5 respectively (Fig. 6A-a2, b2, c2, d2, and B). There were significant statistical differences between Groups WT and LacZ or CMPC ($P < 0.01$) and between Groups CA5 and LacZ or CMPC ($P < 0.01$), but no significant difference between Groups WT and CA5 ($P > 0.05$) (Fig. 6B). At 7 weeks, the percentage of AL labeling (red) was $2.25 \pm 0.66\%$, $1.98 \pm 0.74\%$, $5.05 \pm 0.83\%$, and $7.51 \pm 1.42\%$ respectively (Fig. 6A-a3, b3, c3, d3, and B), with no significant

differences between groups WT and CA5 (Fig. 6B). Taken together, these data indicated that the Lenti-WT and Lenti-CA5 groups could effectively promote new bone formation and mineralization compared with the Lenti-LacZ and CMPC groups. However, there were no significant differences between groups WT and CA5 or between LacZ and CMPC.

3.8. Histological analysis of bone regeneration

Histological evidence of the undecalcified specimens further supported the radiographic and fluorochrome labeling histomorphometrical findings (Fig. 7A). Under light microscopy, the percentage of new bone area after 8 weeks was $25.31 \pm 5.16\%$ in the CA5 group, $23.78 \pm 5.87\%$ in the WT group, $8.63 \pm 7.25\%$ in the LacZ group, and $7.41 \pm 3.54\%$ in the CMPC-alone group, respectively (Fig. 7B). The percentage of remnant scaffold area was $24.52\% \pm 2.41\%$ in the CA5 group, $26.76\% \pm 2.51\%$ in the WT group, $29.61 \pm 2.74\%$ in LacZ group and $33.73\% \pm 2.63\%$ in scaffold-alone group respectively (Fig. 7C).

Concerning the presence of the implanted BMSCs in the defect sites, GFP immunohistochemistry was adopted, because all Lenti-LacZ, Lenti-WT and Lenti-CA5 lentivirus encodes enhanced green fluorescent protein (EGFP). GFP was apparent in the new bone

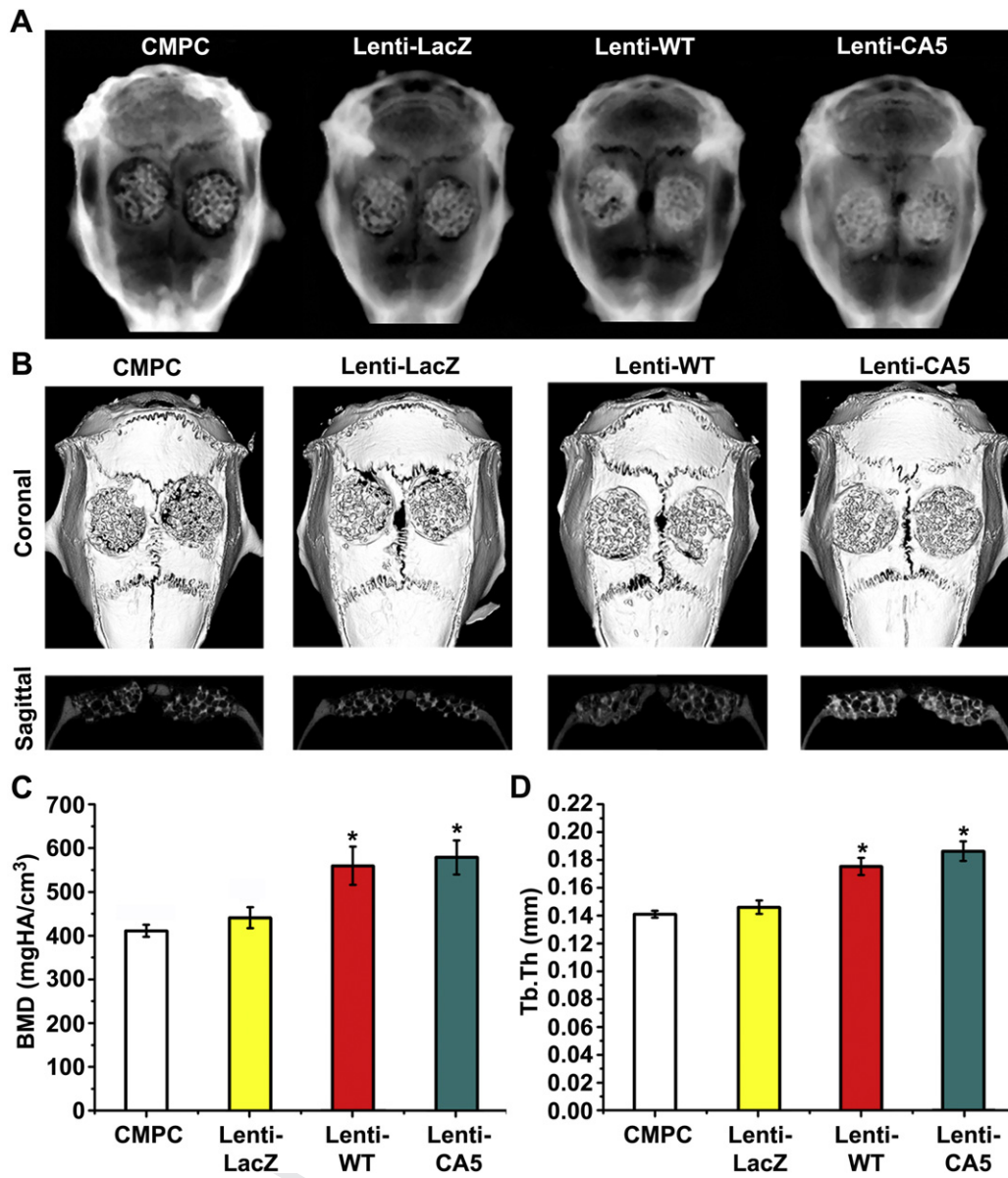


Fig. 5. Radiography and micro-CT evaluation of the repaired skull at 8 weeks after implantation. CMPC constructs, Lenti-LacZ-transduced BMSCs/CMPC constructs, Lenti-WT-transduced BMSCs/CMPC constructs, and Lenti-CA5-transduced BMSCs/CMPC constructs (from left to right). Representative photographs showed large defined radiopacities at the defect sites (A). Micro-CT images of calvarial defects taken 8 weeks after implantation (B). Morphometric analysis of the local bone mineral density in the new bone formation area (C) and the trabecular thickness (D). There were significant differences between the target gene groups and the CMPC or Lenti-LacZ groups (* $P < 0.05$, target gene groups compared with the LacZ group or CMPC group).

matrix or fibrous tissue in the WT-, CA5- and LacZ-transduced BMSCs groups (Fig. 8a) 8 weeks post-operation, while negative staining was found in the CMPC group. Immunohistochemistry displayed intensive HIF-1 α staining in cells both the bone matrix and the surrounding fibroblastic-like tissue for samples treated with the Lenti-WT and Lenti-CA5-transduced BMSCs (Fig. 8b), whereas in Lenti-LacZ-transduced BMSCs and the scaffold-alone groups, there was no obvious positive staining for endogenous HIF-1 α .

4. Discussion

The combination of tissue engineering and gene therapy is a promising strategy for bone regeneration [1]. This study investigated a therapeutic strategy based on CA5-transduced BMSCs in healing a critical-sized cranial defect with CMPC scaffold.

Many studies have demonstrated that the HIF-1 α protein is subject to degradation under normoxic conditions [38]. To effectively maintain the stability and activity of HIF-1 α under non-hypoxic conditions, a constitutively active form of HIF-1 α was constructed. To prevent HIF-1 α proline residues 402 and 564 from hydroxylation and degradation, we made a deletion (amino acids 392–520) and two substitutions (Pro567Thr and Pro658Gln). The deletion stabilized HIF-1 α by preventing it from combining with von Hippel-Lindau protein (VHL) and being degraded. Mutating proline residue 567 to threonine and proline residue 658 to glutamine enhanced HIF-1 α binding to the transcriptional co-activators CBP and p300 to effectively maintain activity in normoxic conditions. The mRNA and protein expression of HIF-1 α in BMSCs transduced with Lenti-CA5 achieved the greatest value among three groups *in vitro*. These data supported that CA5 could effectively maintain the stability and activity of HIF-1 α in normoxic conditions.

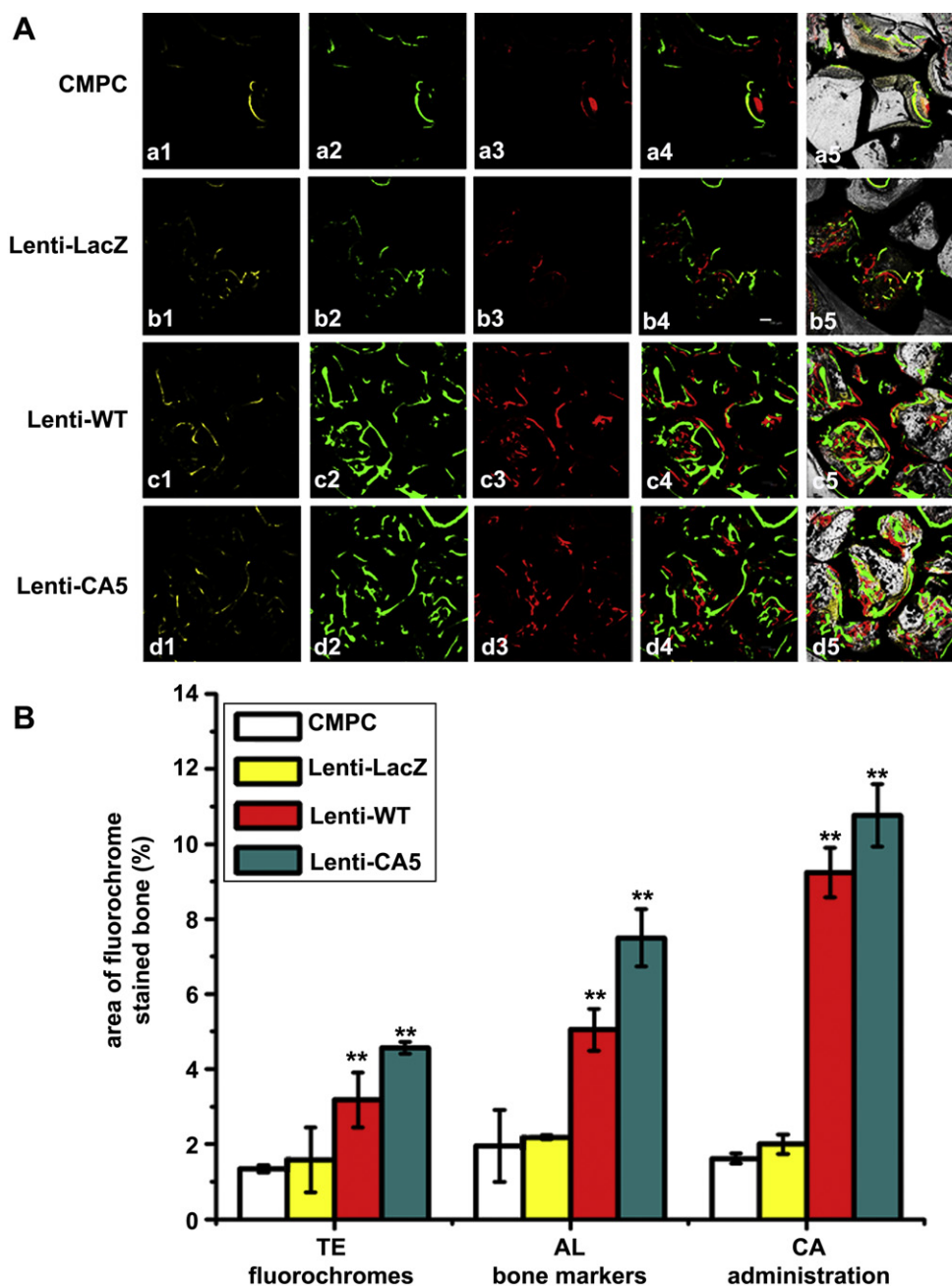


Fig. 6. New bone formation and mineralization was determined histomorphometrically by TE, CA, and AL fluorescent quantification, which represented the mineralization level at 8 weeks after operation (A). Parts a, b, c, and d represent confocal LASER microscope for each group. Parts a4, b4, c4, and d4 represent merged images of the three fluorochromes for the same group. Parts a5, b5, c5, and d5 represent the merged images of the three fluorochromes together with the plain confocal laser microscope image for the same group; (B) The graph shows the percentage of each fluorochrome area for different groups. There were significant differences between the Lenti-WT or Lenti-CA5 groups and the CMPC or Lenti-LacZ groups (** $P < 0.01$, target gene groups compared with the LacZ group or CMPC group).

Some studies have suggested that HIF-1 α might play important roles in bone formation [4]. HIF-1 α is expected to be beneficial when used in gene-modified stem cells for bone regeneration since it belongs to a gene upstream of some factors, including VEGF, SDF-1, TGF- β , and Clut1 [39,40]. To test our hypothesis, the mRNA expression levels of a few key osteogenic factors and the protein expression of four important osteogenic factors were detected in gene-modified BMSCs *in vitro*. Our results demonstrated that Lenti-WT and Lenti-CA5 could induce the overexpression of these osteogenic genes *in vitro* even in a normoxic state. BMP-2 and Cbfa1, both regarded as key osteogenic factors with the strongest and

most significant biological activities which are effective in enhancing bone formation in a variety of animal studies [41], were remarkably upregulated in target gene-treated BMSCs groups at both mRNA and protein levels. In particular, the expression of BMP-2 showed the greatest response, with 30- to 67-fold increases on day 21. This tendency showed that HIF-1 α can induce significant osteogenesis of BMSCs *in vitro*. Moreover, other important factors, such as ALP, Glut1, COL1, osteonectin, OCN, OPN, and BSP, were also significantly upregulated in target gene-transduced groups. The results of ALP and ARS confirmed that CA5-overexpressing BMSCs could induce osteogenesis *in vitro* under non-hypoxic conditions.

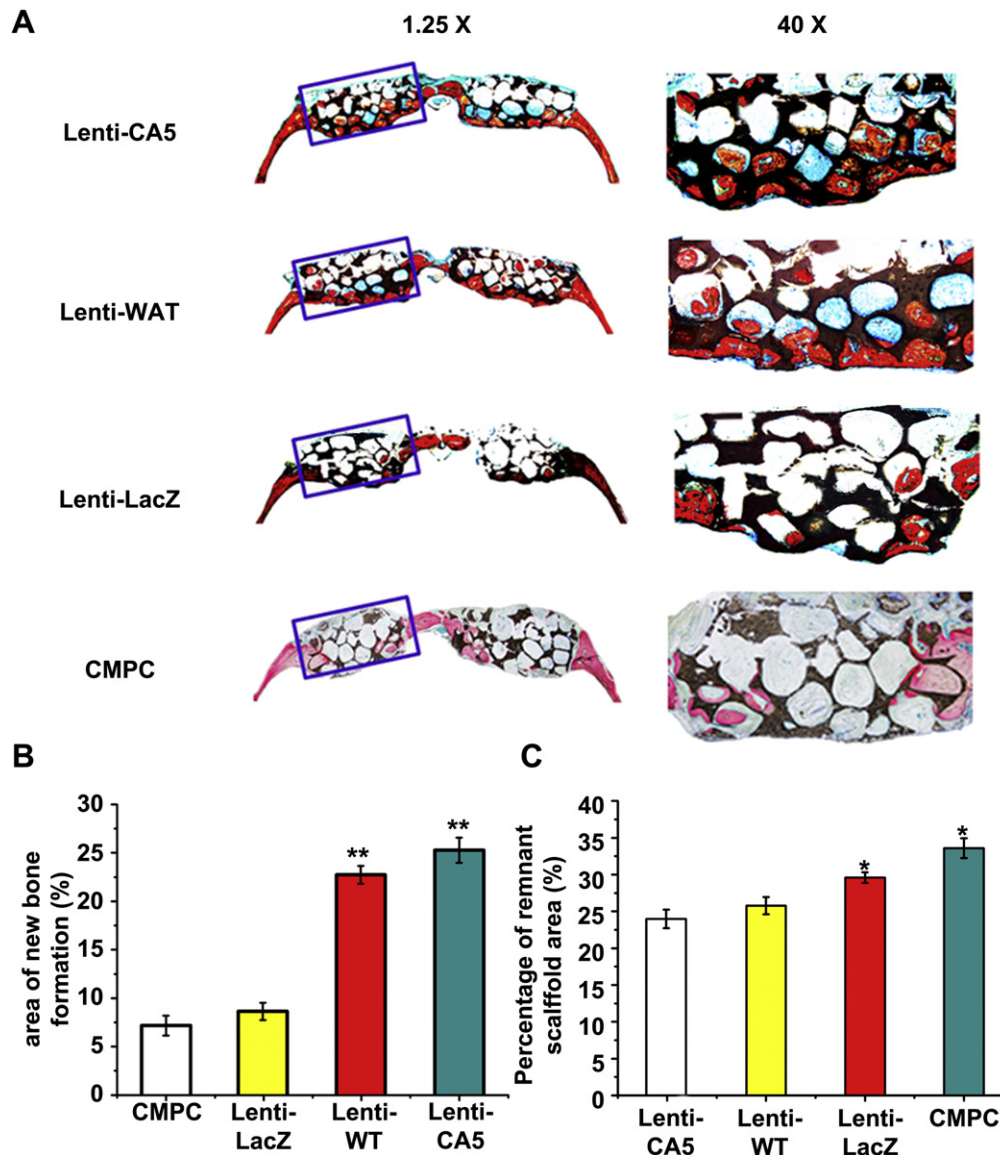


Fig. 7. Histological analysis of newly formed bone and remnant scaffold area in calvarial defects. The specimens were sliced, and sections were stained with van Gieson's picro fuchsin. From top to bottom: CMPC constructs, Lenti-LacZ-transduced BMSCs/CMPC constructs, Lenti-WT-transduced BMSCs/CMPC constructs, and Lenti-CA5-transduced BMSCs/CMPC constructs (original magnification, 1.25 \times , 40 \times) (A). New bone formation area per 40 \times field in sections (B). There were significant differences between the WT or CA5 groups and the CMPC or LacZ groups (** $P < 0.01$, target gene groups compared with the LacZ group or CMPC group). Remnant scaffold area per 40 \times field in sections (C). There were obviously differences between the WT or CA5 groups and the CMPC or LacZ groups (* $P < 0.05$, target gene groups compared with the LacZ group or CMPC group).

Comparing to the function of point mutant HIF-1 α on BMSCs presented in our previous publication [16], CA5 demonstrated higher stability of HIF-1 α in normoxic conditions, at both mRNA and protein levels. Furthermore, the expression of osteogenic markers was stronger in the CA5 group than that of point mutant group including BMP-2, Cbfa1, and OCN. These data suggested that the truncation mutant HIF-1 α gene-modified BMSCs achieved better osteogenic function than that of point mutant HIF-1 α *in vitro* we previously presented. This lead us to further explore its effects in bone repair in animal models.

Lenti-WT and Lenti-CA5 BMSCs were combined with CMPC scaffold to repair bone defects in a critical-sized cranial defect rat model. Due to the advantages in shorter setting time, biocompatibility, and markedly better mechanical properties, CMPC has been regarded as a promising scaffold for bone regeneration [42]. The study showed that Lenti-WT and Lenti-CA5 treatment could significantly improve ossification in calvarial models through the

application of BMSCs. Radiological evaluation revealed that the wild-type and the truncation mutant HIF-1 α -transduced cells could enhance the repair of the defect area. In contrast, only slight new bone formation was observed in the LacZ and CMPC groups. Quantitative analysis by micro-CT revealed newly formed bone in the target gene-transduced groups was much higher than that in the control group at both BMD and Tb.Th. However, CA5 group achieved the greatest effect of bone repair among four groups. In consistent with the above findings, histological examination demonstrated that newly formed bone completely covered the defect area with the implantation of CA5-transduced BMSCs, while there was only limited new bone formation in the control group. The percentage of new bone area was the largest in the CA5 group (25.31 \pm 5.16%) comparing to the WT group (23.78 \pm 5.87%), the LacZ group (8.63 \pm 7.25%), and the CMPC-alone group (7.41 \pm 3.54%). As for the origin and role of the implanted BMSCs, the GFP reporter gene expression in Lenti-LacZ-, Lenti-WT-, and

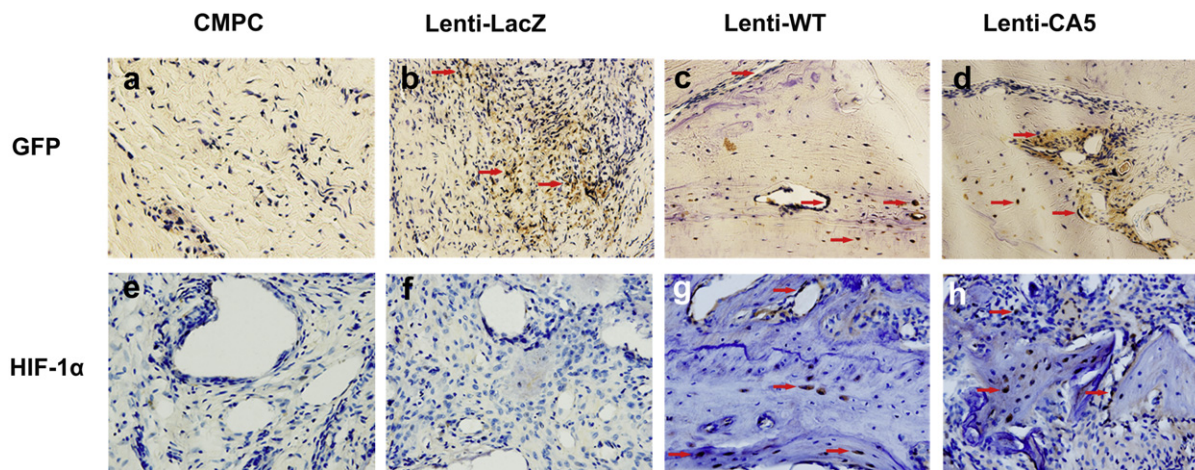


Fig. 8. Immunohistochemical analysis of new bone formation in each group at 8 weeks post-operation. Immunostaining for GFP of (a) scaffold-alone group, (b) Lenti-LacZ group, (c) Lenti-WT group, and (d) Lenti-CA5 group. The LacZ, WT, and CA5 groups show positive brown staining in fibroblastic-like tissue and bone matrix (red arrow). HIF-1 α staining demonstrates strong HIF-1 α expression in both the bone and the surrounding fibroblastic-like tissue (red arrows) in (g) Lenti-WT group and (h) Lenti-CA5 group. There was no obvious positive staining in (e) the scaffold-alone group or (f) the Lenti-LacZ group (a–h, 400 \times). (For interpretation of the references to colour in this figure legend, the reader is referred to the web version of this article.)

Lenti-CA5-transduced groups and the stronger HIF-1 α -positive staining in the CA5- and WT-transduced groups suggested that those donor cells had participated in the new bone formation. Thus, the HIF-1 α gene can effectively induce BMSCs to produce new bone in bone defects *in vivo*. Furthermore, CA5 modified BMSCs group achieved better result of the repair of CSD compared with WT groups.

In this study, the degradation of implanted CMPC scaffold materials was observed obviously but with different patterns in those four groups. CMPC material demonstrated an accelerated degradation in CA5 and WT groups, accompanying with more new bone formation as compared to LacZ group or CMPC alone. The trend is more obvious for CA5-transduced group in which the largest newly formed bone area as well as the fastest CMPC degradation rate were found among the groups. The previous studies have suggested the degradation of CPC materials could be due to osteoclast-mediated degradation [43]. Porous CPC could create a permissive micro-environment of bone formation and mineral resorption, such as the presence of osteoblasts and extracellular matrix (ECM), which could facilitate osteoclasts adhesion via different pathways [44,45]. CMPC, which was derived from CPC, should go through similar mechanism for the degradation of implanted scaffold materials. However, the *in-depth* mechanism concerning to the degradation of materials would be evaluated with longer observation time in larger animal models study in the future.

One report has showed AdHIF-1 α had been used to treat the lower extremity of patients with critical limb ischemia [46]. In our study, we do not find any evidence that the HIF-1 α -overexpressing BMSCs formed tumor during the 8 weeks observation *in vivo*. Of course, a prolonged observation *in vivo* must be considered to determine whether HIF-1 α is safe if we use CA5 as a means of clinical treatment in the future.

5. Conclusions

In summary, BMSCs modified by truncation mutant HIF-1 α gene can promote osteogenesis *in vitro* and *in vivo*. CMPC could serve as a potential substrate for HIF-1 α gene-modified tissue engineered bone for bone regeneration. This work provided more options to further detect the role of HIF-1 α in repairing large bone defect with different mutant methods in the future.

Acknowledgments

The authors appreciate Xiuli Zhang, Chao Zhu, Jun Zhao, and Dongxia Ye for helping animal studies and data collection. This work was supported by the National Natural Science Foundation of China (81070806, 81070864, 81100788), NCET-08-0353, Science and Technology Commission of Shanghai Municipality (09411954800, 10JC1413300, 0952nm04000, 10430710900, 10dz2211600), Science and Technology Commission of Anhui Municipality (11040606M173, 11040606M204), Key Project of Education Department of Anhui Province (KJ2009A037), the Shanghai Municipal Health Bureau for Youth Fund (2009Y082). The authors indicate no potential conflicts of interest.

Appendix. Supplementary data

Supplementary data related to this article can be found online at doi:10.1016/j.biomaterials.2011.09.005.

References

- Bruder SP, Fox BS. Tissue engineering of bone. *Cell Based Strategies Clin Orthop Relat Res* 1999;367(Suppl.):S68–83.
- Xiao C, Zhou H, Liu G, Zhang P, Fu Y, Gu P, et al. Bone marrow stromal cells with a combined expression of BMP-2 and VEGF-165 enhanced bone regeneration. *Biomed Mater* 2011;6(1):015013.
- Qu D, Li J, Li Y, Gao Y, Zuo Y, Hsu Y, et al. Angiogenesis and osteogenesis enhanced by bFGF ex vivo gene therapy for bone tissue engineering in reconstruction of calvarial defects. *J Biomed Mater Res A* 2011;96(3):543–51.
- Wang Y, Wan C, Deng L, Liu X, Cao X, Gilbert SR, et al. The hypoxia-inducible factor alpha pathway couples angiogenesis to osteogenesis during skeletal development. *J Clin Invest* 2007;117(6):1616–26.
- Ivan M, Kondo K, Yang H, Kim W, Valiando J, Ohh M, et al. HIF1alpha targeted for VHL-mediated destruction by proline hydroxylation: implications for O₂ sensing. *Science* 2001;292(5516):464–8.
- Semenza GL. Regulation of mammalian O₂ homeostasis by hypoxia-inducible factor 1. *Annu Rev Cell Dev Biol* 1999;15:551–78.
- Lando D, Peet DJ, Gorman JJ, Whelan DA, Whitelaw ML, Bruckner RK. FIH-1 is an asparaginyl hydroxylase enzyme that regulates the transcriptional activity of hypoxia-inducible factor. *Genes Dev* 2002;16(12):1466–71.
- Bruick RK, McKnight SL. A conserved family of prolyl-4-hydroxylases that modify HIF. *Science* 2001;294(5545):1337–40.
- Epstein AC, Gleadle JM, McNeill LA, Hewitson KS, O'Rourke J, Mole DR, et al. C. elegans EGL-9 and mammalian homologs define a family of dioxygenases that regulate HIF by prolyl hydroxylation. *Cell* 2001;107(1):43–54.
- Jaakkola P, Mole DR, Tian YM, Wilson MI, Gielbert J, Gaskell SJ, et al. Targeting of HIF-1alpha to the von Hippel-Lindau ubiquitylation complex by O₂-regulated prolyl hydroxylation. *Science* 2001;292(5516):468–72.

- 1411 [11] Lando D, Peet DJ, Whelan DA, Gorman JJ, Whitelaw ML. Asparagine hydroxy-
1412 lation of the HIF transactivation domain a hypoxic switch. *Science* 2002;
1413 295(5556):858–61. 1454
- 1414 [12] Kelly BD, Hackett SF, Hirota K, Oshima Y, Cai Z, Berg-Dixon S, et al. Cell type-
1415 specific regulation of angiogenic growth factor gene expression and induction
1416 of angiogenesis in nonischemic tissue by a constitutively active form of
1417 hypoxia-inducible factor 1. *Circ Res* 2003;93(11):1074–81. 1455
- 1418 [13] Liechty KW, MacKenzie TC, Shaaban AF, Radu A, Moseley AM, Deans R, et al.
1419 Human mesenchymal stem cells engraft and demonstrate site-specific
1420 differentiation after in utero transplantation in sheep. *Nat Med* 2000;6(11):
1421 1282–6. 1456
- 1422 [14] Tsuda H, Wada T, Ito Y, Uchida H, Dehari H, Nakamura K, et al. Efficient BMP2
1423 gene transfer and bone formation of mesenchymal stem cells by a fiber-
1424 mutant adenoviral vector. *Mol Ther* 2003;7(3):354–65. 1457
- 1425 [15] Zhao Z, Wang Z, Ge C, Krebsbach P, Franceschi RT. Healing cranial defects with
1426 AdRunx2-transduced marrow stromal cells. *J Dent Res* 2007;86(12):1207–11. 1458
- 1427 [16] Zou D, Zhang Z, Ye D, Tang A, Deng L, Han W, et al. Repair of critical-sized rat
1428 calvarial defects using genetically engineered BMSCs overexpressing HIF-
1429 1alpha. *Stem Cells* 2011;29(9):1380–90. 1459
- 1430 [17] Scheller EL, Krebsbach PH, Kohn DH. Tissue engineering: state of the art in
1431 oral rehabilitation. *J Oral Rehabil* 2009;36(5):368–89. 1460
- 1432 [18] Brown WE, Chow LC. Effects of neutral salts in a bench-scale caries model.
1433 *J Dent Res* 1986;65(9):1115–20. 1461
- 1434 [19] Carletti E, Motta A, Migliaresi C. Scaffolds for tissue engineering and 3D cell
1435 culture. *Methods Mol Biol* 2011;695:17–39. 1462
- 1436 [20] Zhang C, Wang KZ, Qiang H, Tang YL, Li Q, Li M, et al. Angiopoiesis and bone
1437 regeneration via co-expression of the hVEGF and hBMP genes from an adeno-
1438 associated viral vector *in vitro* and *in vivo*. *Acta Pharmacol Sin* 2010;31(7):821–30. 1463
- 1439 [21] Ooms EM, Egglezos EA, Wolke JG, Jansen JA. Soft-tissue response to injectable
1440 calcium phosphate cements. *Biomaterials* 2003;24(5):749–57. 1464
- 1441 [22] Bohner M, Theiss F, Apelt D, Hirsiger W, Houriet R, Rizzoli G, et al. Composi-
1442 tional changes of a dicalcium phosphate dihydrate cement after implanta-
1443 tion in sheep. *Biomaterials* 2003;24(20):3463–74. 1465
- 1444 [23] Ogose A, Kondo N, Umezue H, Hotta T, Kawashima H, Tokunaga K, et al.
1445 Histological assessment in grafts of highly purified beta-tricalcium phosphate
1446 (OSferion) in human bones. *Biomaterials* 2006;27(8):1542–9. 1466
- 1447 [24] Wei J, Jia J, Wu F, Wei S, Zhou H, Zhang H, et al. Hierarchically microporous/
1448 macroporous scaffold of magnesium-calcium phosphate for bone tissue
1449 regeneration. *Biomaterials* 2010;31(6):1260–9. 1467
- 1450 [25] Staiger MP, Pietak AM, Huadmai J, Dias G. Magnesium and its alloys as
1451 orthopedic biomaterials: a review. *Biomaterials* 2006;27(9):1728–34. 1468
- 1452 [26] Yamasaki Y, Yoshida Y, Okazaki M, Shimazu A, Kubo T, Akagawa Y, et al.
1453 Action of FGMgCO₃Ap-collagen composite in promoting bone formation.
1454 *Biomaterials* 2003;24(27):4913–20. 1469
- 1455 [27] Kondo N, Ogose A, Tokunaga K, Ito T, Arai K, Kudo N, et al. Bone formation and
1456 resorption of highly purified beta-tricalcium phosphate in the rat femoral
1457 condyle. *Biomaterials* 2005;26(28):5600–8. 1470
- 1458 [28] Edwards PC, Ruggiero S, Fantasia J, Burakoff R, Moorji SM, Paric E, et al. Sonic
1459 hedgehog gene-enhanced tissue engineering for bone regeneration. *Gene
1460 Ther* 2005;12(1):75–86. 1471
- 1461 [29] Jiang X, Zhao J, Wang S, Sun X, Zhang X, Chen J, et al. Mandibular repair in rats
1462 with premineralized silk scaffolds and BMP-2-modified bMSCs. *Biomaterials*
1463 2009;30(27):4522–32. 1472
- 1464 [30] Kasten P, Luginbuhl R, van GM, Barkhausen T, Krettek C, Bohner M, et al.
1465 Comparison of human bone marrow stromal cells seeded on calcium-deficient
1466 hydroxyapatite, beta-tricalcium phosphate and demineralized bone matrix.
1467 *Biomaterials* 2003;24(15):2593–603. 1473
- 1468 [31] Livak KJ, Schmittgen TD. Analysis of relative gene expression data using real-
1469 time quantitative PCR and the 2(-Delta Delta C(T)) method. *Methods* 2001;
1470 25(4):402–8. 1474
- 1471 [32] Mardas N, Stavropoulos A, Karring T. Calvarial bone regeneration by
1472 a combination of natural anorganic bovine-derived hydroxyapatite matrix
1473 coupled with a synthetic cell-binding peptide (PepGen): an experimental
1474 study in rats. *Clin Oral Implants Res* 2008;19(10):1010–5. 1475
- 1475 [33] Roldan JC, Jepsen S, Miller J, Freitag S, Rueger DC, Acil Y, et al. Bone formation
1476 in the presence of platelet-rich plasma vs. bone morphogenetic protein-7.
1477 *Bone* 2004;34(1):80–90. 1476
- 1478 [34] Cacciafesta V, Dalstra M, Bosch C, Melsen B, Andreassen TT. Growth hormone
1479 treatment promotes guided bone regeneration in rat calvarial defects. *Eur J
1480 Orthod* 2001;23(6):733–40. 1477
- 1481 [35] Sun XJ, Zhang ZY, Wang SY, Gittens SA, Jiang XQ, Chou LL. Maxillary sinus floor
1482 elevation using a tissue-engineered bone complex with osteobone and bMSCs
1483 in rabbits. *Clin Oral Implants Res* 2008;19(8):804–13. 1478
- 1484 [36] Wang S, Zhang W, Zhao J, Ye D, Zhu C, Yang Y, et al. Long-term outcome of
1485 cryopreserved bone-derived osteoblasts for bone regeneration *in vivo*.
1486 *Biomaterials* 2011;32(20):4546–55. 1479
- 1487 [37] Wang S, Zhang Z, Zhao J, Zhang X, Sun X, Xia L, et al. Vertical alveolar ridge
1488 augmentation with beta-tricalcium phosphate and autologous osteoblasts in
1489 canine mandible. *Biomaterials* 2009;30(13):2489–98. 1480
- 1490 [38] Compennolle V, Brusselmans K, Franco D, Moorman A, Dewerchin M, Collen D,
1491 et al. Cardia bifida, defective heart development and abnormal neural crest
1492 migration in embryos lacking hypoxia-inducible factor-1alpha. *Cardiovasc Res*
1493 2003;60(3):569–79. 1481
- 1494 [39] Ke Q, Costa M. Hypoxia-inducible factor-1 (HIF-1). *Mol Pharmacol* 2006;70(5):
1495 1469–80. 1482
- 1496 [40] Semenza GL. Hypoxia-inducible factor 1 (HIF-1) pathway. *Sci STKE* 2007;
1497 2007(407):cm8. 1483
- 1498 [41] Majmundar AJ, Wong WJ, Simon MC. Hypoxia-inducible factors and the
1499 response to hypoxic stress. *Mol Cell* 2010;40(2):294–309. 1484
- 1500 [42] Rey S, Semenza GL. Hypoxia-inducible factor-1-dependent mechanisms of
1501 vascularization and vascular remodelling. *Cardiovasc Res* 2010;86(2):236–42. 1485
- 1502 [43] Kroese-Deutman HC, Ruhe PQ, Spauwen PH, Jansen JA. Bone inductive
1503 properties of rhBMP-2 loaded porous calcium phosphate cement implants
1504 inserted at an ectopic site in rabbits. *Biomaterials* 2005;26(10):1131–8. 1486
- 1505 [44] Mastrogiacomo M, Scaglione S, Martinetti R, Dolcini L, Beltrame F, Cancedda R,
1506 et al. Role of scaffold internal structure on *in vivo* bone formation in macro-
1507 porous calcium phosphate bioceramics. *Biomaterials* 2006;27(17):3230–7. 1487
- 1508 [45] Mastrogiacomo M, Papadimitropoulos A, Cedola A, Peyrin F, Giannoni P,
1509 Pearce SG, et al. Engineering of bone using bone marrow stromal cells and
1510 a silicon-stabilized tricalcium phosphate bioceramic: evidence for a coupling
1511 between bone formation and scaffold resorption. *Biomaterials* 2007;28(7):
1512 1376–84. 1488
- 1513 [46] Rajagopalan S, Olin J, Deitcher S, Pieczek A, Laird J, Grossman PM, et al. Use of
1514 a constitutively active hypoxia-inducible factor-1alpha transgene as a thera-
1515 peutic strategy in no-option critical limb ischemia patients: phase I dose-
1516 escalation experience. *Circulation* 2007;115(10):1234–43. 1489